

# Geo-Spatial Dynamics of Land Surface Temperature of Port Harcourt Metropolis and Environs: Implication for Heat Disaster Management

Nwaerema Peace<sup>1,\*</sup>, Temi Emmanuel Ologunorisa<sup>2</sup>, Moses Okemini Nwagbara<sup>3</sup>,  
Ojeh Nduka Vincent<sup>4</sup>

<sup>1</sup>Department of Geography and Environmental Management, University of Port Harcourt, Port Harcourt, Nigeria

<sup>2</sup>Department of Meteorology and Climate Science, Federal University of Technology, Akure, Nigeria

<sup>3</sup>Department of Soil Science and Meteorology, Michael Okpara University of Agriculture, Umuahia, Nigeria

<sup>4</sup>Department of Geography, Taraba State University, Jalingo, Nigeria

## Email address:

pnwaerema486@gmail.com (N. Peace), ologunorisa1966@gmail.com (T. E. Ologunorisa), monwagbara@gmail.com (M. O. Nwagbara),  
drojehvn@tsuniversity.edu.ng (O. N. Vincent)

\*Corresponding author

## To cite this article:

Nwaerema Peace, Temi Emmanuel Ologunorisa, Moses Okemini Nwagbara, Ojeh Nduka Vincent. Geo-Spatial Dynamics of Land Surface Temperature of Port Harcourt Metropolis and Environs: Implication for Heat Disaster Management. *Earth Sciences*. Vol. 8, No. 3, 2019, pp. 169-177. doi: 10.11648/j.earth.20190803.15

**Received:** May 12, 2019; **Accepted:** June 13, 2019; **Published:** June 26, 2019

---

**Abstract:** Since 1986, the rate of expansion of population and urban pavement materials in Port Harcourt metropolis and environs has generated enormous heat capable of causing disaster. This paper examines geo-spatial dynamics of Land Surface Temperature (LST) of Port Harcourt metropolis and environs from 1986 to 2018 using Geographic Information Systems (GIS) approach. To achieve this purpose, satellite data were retrieved and analyzed using the algorithm for extracting LST from Landsat 5, 7 and 8 thermal infrared sensor sources from the Google Earth Engine (GEE). The results indicate that in 1986, LST concentrated on the south-western (Bakana) and north-eastern (Oyigbo) sections of the city with temperature range of 19.27°C and 30.17°C having population of 757,022 persons. In 2003, LST concentrated on the city centre, south-western (Bakana) and north-western (Rumuekeni) segments with temperature range of 16.14°C and 34.19°C having population of 1,143,103 persons respectively. Also, in 2018 LST shifted its concentration to north-eastern and south-eastern segments of the city with a variation of 21.6°C and 35.31°C having population of 3,095,342 persons expected to experience heat related ailments such as heat stroke. The city has compromised the standard human comfort threshold of 27°C. It is recommended that there should be immediate urban greening of tree planting, de-congestion of development activities from the eastern segment of Port Harcourt city to the western segment as well as practical implementation of urban management plan without further delay.

**Keywords:** Geo-spatial, GIS, Land Surface Temperature, Urban Pavement Materials, Population, Heat Disaster

---

## 1. Introduction

Due to increased population, urban pavement materials of Port Harcourt metropolis and environs have increased and modified the natural spatial features of the city. From colonial time, Port Harcourt has continued to expand its landscape and swallowing undeveloped plots of land and transforming the land use types. Thus, during the early 1980s Port Harcourt city has drawn much attention to researchers

due to increased structural transformation caused by population and economic growth resulting to high thermal activity of the city in the form of Land Surface Temperature (LST) [1].

Land Surface Temperature (LST) is a measure of heat radiated or emitted from urban fabrics due to different anthropogenic activities taking place on the land surface [2]. Conceived land surface temperature as the perceived hotness of a surface from the satellite point. LST of objects is distinct

from temperature of air. Temperature of different states of matter whether solid, liquid or gas on the ground surface varies according to location and climatic parameters as well as human activities. Increased in pavement materials is an indication of rise in man's activities to the land surface which results to land surface temperature [3]. From the city center to the fringes of a city, land surface temperature varies according to different land use types [4]. Over time as human activities in a city begin to increase, land use land cover invariably reduces thereby giving way to LST which alters the regional climate of the area [5]. Many studies have revealed changes in the water cycle and general evapotranspiration processes due to large scale biophysical alteration of the city surface areas [6, 7].

When the LST of a city is compromised, there will be high demand of energy, increased pollutants reaction, rise in greenhouse gas effect, health disaster and low water quality. In the city, there are many parameters that have brought about LST rise such as loss of urban tree cover, emission of greenhouse gas, increased pavement surfaces and low albedo of materials; others are thermal properties of materials, urban morphology, city size and generated anthropogenic heat [8]. With rapid urbanization in the city, there is increased pressure on land thereby altering the vegetal and water bodies particularly in the fringes resulting to serious heat effect.

In recent time, geo-spatial technologies such as remote sensing (RS) and geographic information systems (GIS) have become effective instruments for monitoring the trend, pattern and magnitude of LST for long term planning and management of urban heat. Various urban fabrics consume insolation and radiate energy from land surface resulting to atmospheric temperature rise which have a high heat capacity and conductivity due to vegetation and water surfaces. This temperature rise can be monitored using space borne remote sensing process in the form of Top of the Atmosphere (TOA) radiances in the Thermal Infrared (TIR) region [9]. The TOA radiance is the net radiance from the earth's surface as upsurge radiance from the atmosphere and downside radiance from the sky. The brightness temperatures known as the blackbody temperatures are retrieved from the TOA radiance [10]. The brightness temperatures account for various properties of the land surface such as the quantity and nature of vegetation cover and thermal properties as well as moisture content of the soil [11]. It is on this background that this investigation was carried out to examine geo-spatial dynamics of land surface temperature of Port Harcourt metropolis and environs in order to understand the implication of LST in heat disaster management for sustainable living environment.

## 2. Materials and Method

### 2.1. The Description of Study Area

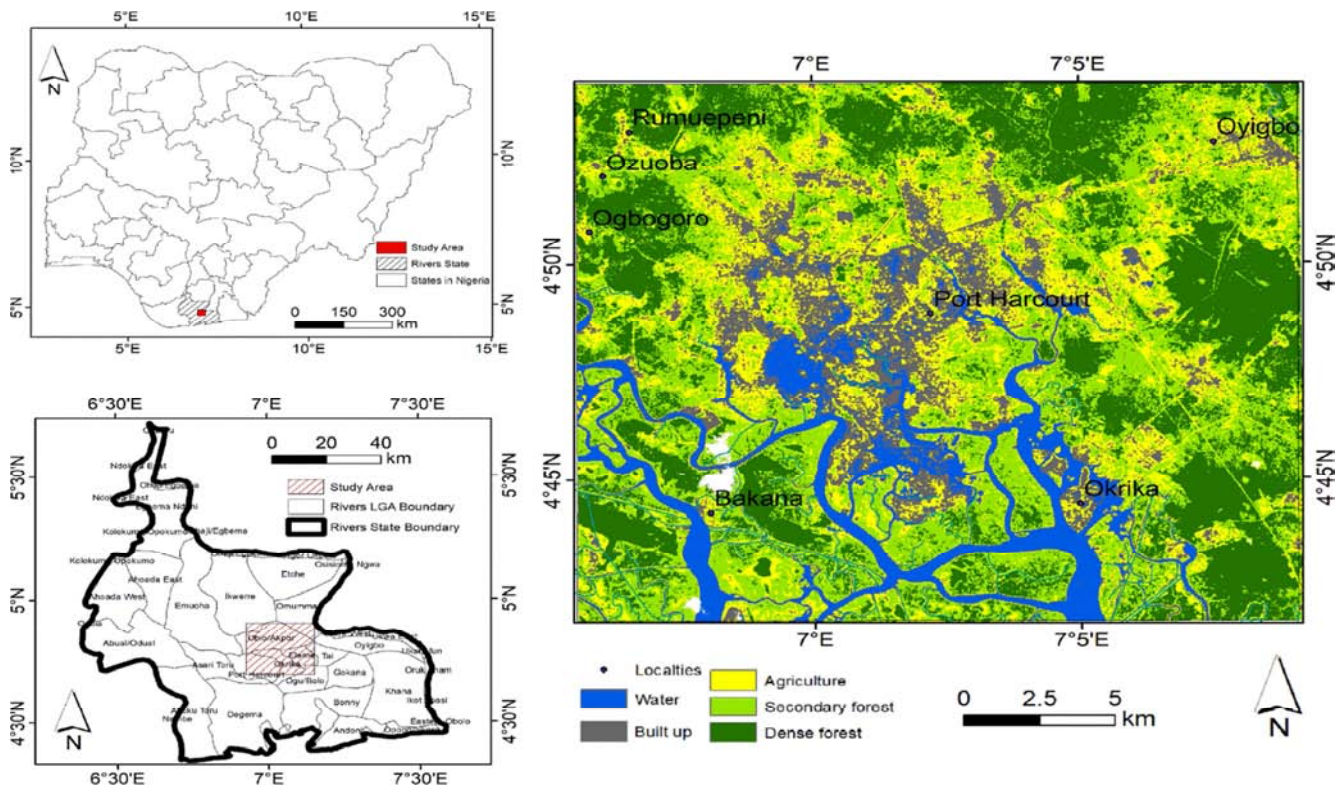


Figure 1. Study Area (Port Harcourt Metropolis and Environs).



Figure 2. Rivers State showing Port Harcourt Metropolis and Environs.

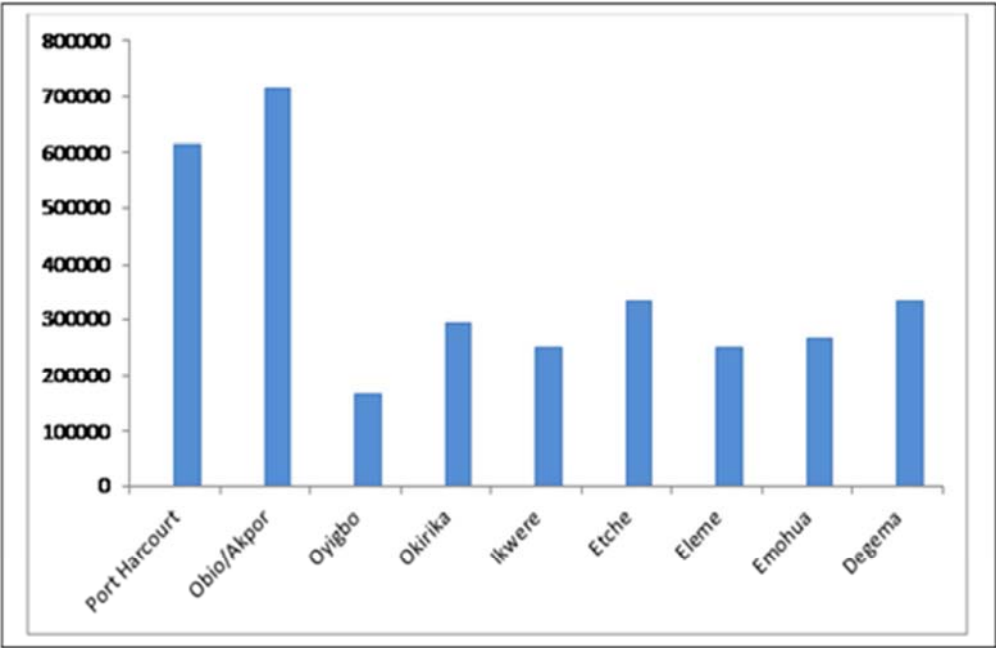


Figure 3. Population of Port Harcourt City and surrounding LGAs.

Port Harcourt metropolis and environs is lying approximately within longitude 70°E and 70°5 E and latitude 4045°N and 4050 N of the GMT (Figure 1). The space encompasses Obio/Akpor and Port Harcourt City LGAs; and extends to the environs of Eleme, Degema, Oyibo, Emohua, Etche, Okirika and Ikwerre LGAs respectively (Figure 2). Due to urban growth, these LGAs are clustered as one metropolis. Obio/Akpor and Port Harcourt City LGAs make up the major urban center; the remaining LGAs have sub-urban and rural characteristics. Additionally, Port Harcourt city and environs remains in recent times the largest area in population with 3,095,342 persons (Figure 3) within the South-South geopolitical zone of Nigeria amongst the six states namely: Cross Rivers, Akwa Ibom, Rivers, Bayelsa, Delta and Edo respectively.

Port Harcourt and its environs is located at the coastal extension of the Atlantic Ocean in the Niger Delta Region of Nigeria influenced by the equatorial monsoon climate. The maritime and continental air masses cause rainfall and temperature pattern of the city [12]. As a city located in the Inter-Tropical Convergence Zone (ITCZ) of Africa, the humid maritime tropical air mass, south-western winds as well as the hot and dry continental air masses from the north-easterly winds characterize its climatic condition. The moist westerly wind produces heavy rainfall volumes of 2000mm to 2500mm with the peak period from April to October [13]. The wet season begins from April when the relative humidity rises and top in July to September, gradually dropping steadily till March with the lowest occurrence in January [14]. In a year cycle, the city temperature rises in January to March and relative humidity decreases continuously resulting to the extreme dry season. LST is a function of surface temperature relative humidity

and wind flow systems. The area experiences average temperature of 35.3°C and 26°C in January and July respectively [15]. Being a coastal settlement, Port Harcourt metropolis and environs has high humidity of 85% during the wet season and lower during the dry season [16]. Cloud cover steadily increases with monthly average of over 6 oktas due to the massive water vapor that rises to the atmosphere as a result of adjacent water bodies from the Atlantic Ocean [15]. Wet months recorded the highest cloud cover and the dry months have the lowest with average daily sunshine of less than 3 hours (wet season) as observed in July and about 4 to 5 hours in months of January and December respectively [17]. The wind pattern varies with mean monthly range of 0-3m/s with high and low trends observed during the nocturnal hours [18, 19]. Land surface temperature in Port Harcourt Metropolis and Environs, Rivers State, Nigeria is characterized by these meteorological variables.

## 2.2. Methods of Data Collection

For satellite data retrieval and analysis, the algorithm for extracting LST from Landsat 5, 7 and 8 thermal infrared sensors, using different surface emissivity sources from the Google Earth Engine (GEE) which is an advanced earth science data and analysis platform allows the estimation of LST products from any part of the globe, covering the time period from 1986, 2003 and 2018 was applied. GEE offers easy and instant access to satellite data, easy to compute and process directly on the platform without need for download. The Landsat 5, 7 and 8 satellites carry thermal infrared radiometers which allows data suitable for LST estimation. The date of retrieval, satellite sensor and pathway are as in Table 1.

Table 1. Details of Landsat Data Retrieved.

Dates of Retrieval	Satellite/Sensor	Reference System/Path/Row
01/01/16 - 30/01/16	GEE/Landsat 5/7/8	AoI
01/01/02 – 30/01/02	GEE/Landsat 5/7/8	AoI
01/01/86 – 30/01/86	GEE/Landsat 5/7/8	AoI

A Single Channel (SC) algorithm was used for consistency among the estimated LST products and option of using emissivity from different points allows flexibility for the algorithm's performance. Among the three Landsat of 5, 7 and 8, it is only Landsat 8 that carries two thermal bands therefore the SC approach was used for consistency. The Landsat 5 archive extends from March 1984 to May 2012, the Landsat 7 archive extends from May 1999 to present and the Landsat 8 archive from April 2013 to present day [20].

The SC algorithm method was used to analyze Landsat 5, 7 and 8 thermal infrared observations. The LST estimation performed using the Google cloud computing servers, with direct access to the GEE satellite data catalogue. Using a SC approach, the LST ( $T_s$ ) can be calculated from the radiance-at-the-sensor in a single band using the radiative transfer equation as follows:

$$LST = Y \left[ \frac{1}{\epsilon} (\psi_1 \cdot L_{sen} + \psi_2 + \psi_3) \right] + \delta \quad (1)$$

Where,

$$Y = \left[ \frac{C_2 \cdot L_{sen}}{T_b^2} \cdot \left[ (\lambda^4 \cdot L_{sen}) / C_1 + 1/\lambda \right] \right] - 1 \quad (2)$$

$$\delta = -y L_{sen} + Tb \quad (3)$$

$$\psi = C \cdot \begin{Bmatrix} PW^2 \\ PW \\ 1 \end{Bmatrix} \rightarrow \begin{Bmatrix} \psi_1 \\ \psi_2 \\ \psi_3 \end{Bmatrix} \begin{Bmatrix} C_{11} & C_{12} & C_{13} \\ C_{12} & C_{22} & C_{23} \\ C_{31} & C_{32} & C_{33} \end{Bmatrix} \cdot \begin{Bmatrix} PW_2 \\ PW \\ 1 \end{Bmatrix} \quad (4)$$

Where Planck's constant value  $c_1$  is  $1.19104 \times 10^8 \text{ W } \mu\text{m}^4 \text{ m}^{-2} \text{ sr}^{-1}$  and  $C_2$  is  $14,387.7 \text{ } \mu\text{m K}$ ;  $\lambda$  is the central wavelength of the thermal band of the Landsat sensor in question;  $L_{sen}$  in  $\text{W sr}^{-1} \text{ m}^{-2} \mu\text{m}^{-1}$ ;  $T_b$  is the brightness

temperature in Kelvin;  $C$  is the coefficients table, with  $c_{ij}$  derived by simulations using different atmospheric profiles and  $\psi x$  is the coefficients weighted with PW.

In order to achieve the product of the Landsat Thermal Radiance-at-Sensor, the level 1T (precision Ortho-corrected) products for each Landsat stage provided by the USGS were orthorectified images of the thermal infrared radiance-at-the-sensor. These satellite products were available in the like of an image collection for each Landsat in the GEE catalogue. The images at different collection points possess digital number values, which were converted to radiance-at-sensor through GEE function using the scaling factors. Notably, the Landsat thermal bands were of varied spatial resolutions which have high reliability among different Landsat sensors as all derived products were resampled by the USGS up to  $30\text{ m} \times 30\text{ m}$  by applying a cubic convolution resampling method [21].

By directly inverting the Planck function, the brightness temperature was estimated. The GEE catalogue possess image collection of Landsat top-of-the-atmosphere (TOA) brightness temperature. The Landsat brightness temperature product in the GEE catalogue contains cloud cover information which can be derived using the Fmask approach. The Fmask is a good method for spotting clouds, cloud shadows, water surfaces and others in Landsat imagery. The brightness temperature and information on the clouds, cloud shadows and water surfaces were used for image collections. The Landsat surface reflectance was available through the GEE catalogue, in the form of image collections. The red and near-infrared bands were used for the calculation of the NDVI, which was needed in order to estimate the NDVI-based emissivity and LST [22].

Emissivity was introduced for LST estimation, since error in emissivity of 1% can result to noticeable errors in the LST to the value of 1 K depending sensor setting, climatological and geographical conditions of the area. For this reason, three different sources of emissivity of ASTER and MODIS in GEE and NDVI-based emissivity estimated from Landsat red and near-infrared data. The reason was to test their strengths and weaknesses was to compare their impact on the LST retrieval for different land types, corresponding to different landscapes and ecosystems. Fraction of vegetation cover (FVC) was estimated using Equation (6), by assuming the NDVI threshold for non-vegetated ( $NDVI_{nonveg}$ ) and vegetated ( $NDVI_{veg}$ ) surfaces to be 0.18 and 0.85, respectively. Emissivity was estimated using Equation (7), assuming a reference emissivity for non-vegetated ( $\epsilon_{nonveg}$ ) and vegetated surfaces ( $\epsilon_{veg}$ ) to be 0.97 and 0.99, respectively. The NDVI-based emissivity product was of  $30\text{ m} \times 30\text{ m}$  spatial resolution, matching exactly the Landsat thermal data [23]. The following formulas were applied:

$$FVC = \left[ \frac{NDVI - NDVI_{nonveg}}{NDVI_{veg} - NDVI_{nonveg}} \right] 2 \quad (5)$$

$$\epsilon = \epsilon_{nonveg} \cdot (1 - FVC) + \epsilon_{veg} \cdot FVC \quad (6)$$

### 3. Results and Discussion

In 1986 (Figure 4 and Table 2), Land surface temperature had high temperature of  $30.17^{\circ}\text{C}$  and low temperature of  $19.27^{\circ}\text{C}$  ranging  $10.9^{\circ}\text{C}$ . LST concentrated on the south-western (Bakana) segment of Port Harcourt to the center of the city. Also, LST had high intensity in the south-eastern (Okirika) segment. The southern part of the city extends to the Atlantic Ocean with temperature as low as  $19.27^{\circ}\text{C}$  as it was dominated by water bodies. The north-eastern (Oyigbo) segment of the city had high concentration of LST. The north-eastern (Rumuekeni) and eastern parts of the city experienced low LST. The spatial distribution of LST in Port Harcourt metropolis and environs is a function of variation of urban fabrics and general anthropogenic activities. It shows, therefore that in 1986, human activities generating LST were more in the south-western and north-western sections respectively. There was intense LST in some parcels of land types across the city surface area.

In 2003 (Figure 5 and Table 2), LST varied between  $16.1^{\circ}\text{C}$  and  $34.2^{\circ}\text{C}$  ranging  $18.1^{\circ}\text{C}$  indicating the highest LST growth. This year recorded relatively the coolest LST; and land surface temperature concentrated more on the center of the city and decreased toward the outskirts. Thus, LST increased in the north-western (Rumuekeni) segment of the city environs. The south-eastern (Okirika) section remained low LST due to high water body and vegetal cover. In this year, the north-eastern (Oyigbo) segment of the city environs recorded low concentration of LST seemingly caused by poor urban infrastructure. Generally, urban growth in Port Harcourt metropolis and environs concentrated on the south-western (Bakana) direction during this period.

In 2018 (Figure 6 and Table 2), land surface temperature varied between  $35.31^{\circ}\text{C}$  and  $21.6^{\circ}\text{C}$  with a range of  $13.5^{\circ}\text{C}$  indicating the highest range of LST. Thus, LST increasingly spread toward the north-eastern direction of Oyibo indicating area of high urban pavement material concentration and growth. LST was low in Bakana and Okirika area (Figure 5). The low land surface temperature of Port Harcourt Metropolis and Environs in the southern segment was due to increased vegetal and water body concentration. The north-eastern section (Rumuekeni) had reduced LST which seem to be influenced by low urban fabric concentration of buildings and general anthropogenic activities. The north-eastern (Oyigbo) with  $35.31^{\circ}\text{C}$  was susceptible to heat disaster due to intense concentration of LST and extended distance from the Atlantic Ocean, low vegetation and water bodies.

**Table 2.** Area Concentration and Direction of LST over the Study Years.

Year	LST Level ( $^{\circ}\text{C}$ )	Area Concentration and Direction of LST
2018	21.60 -35.31	City center and north-eastern (Oyigbo) areas.
2003	16.14-34.19	City center, south-western (Bakana) and north-western (Rumuekeni) areas.
1986	19.27- 30.17	City center, south-western (Bakana) and north-eastern (Oyibo) areas.



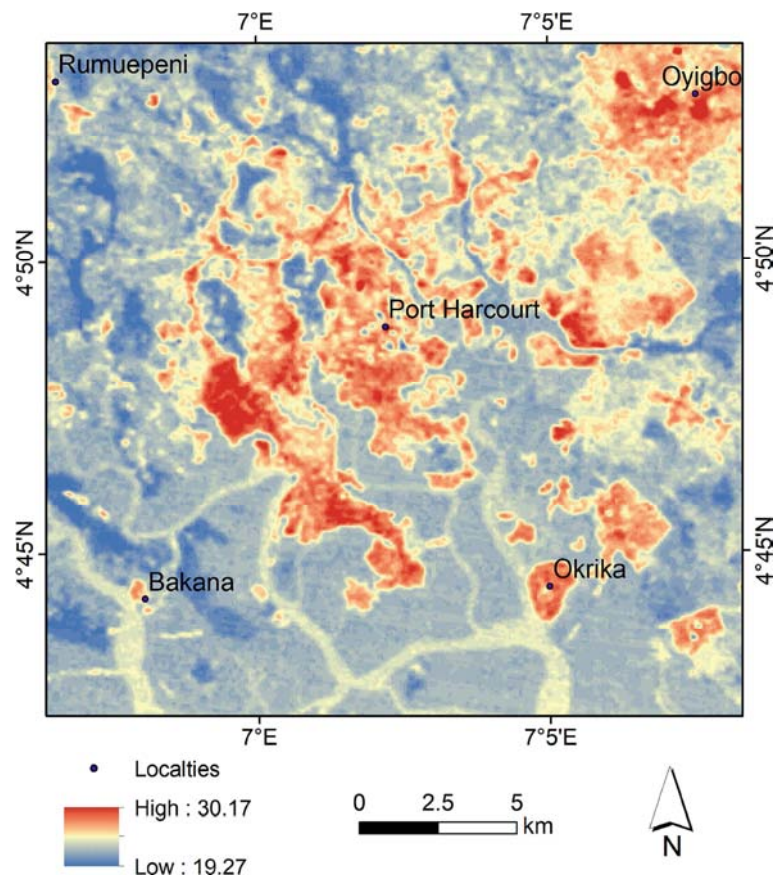


**Figure 4.** Land Surface Temperature of Port Harcourt Metropolis and Environs, 1986.

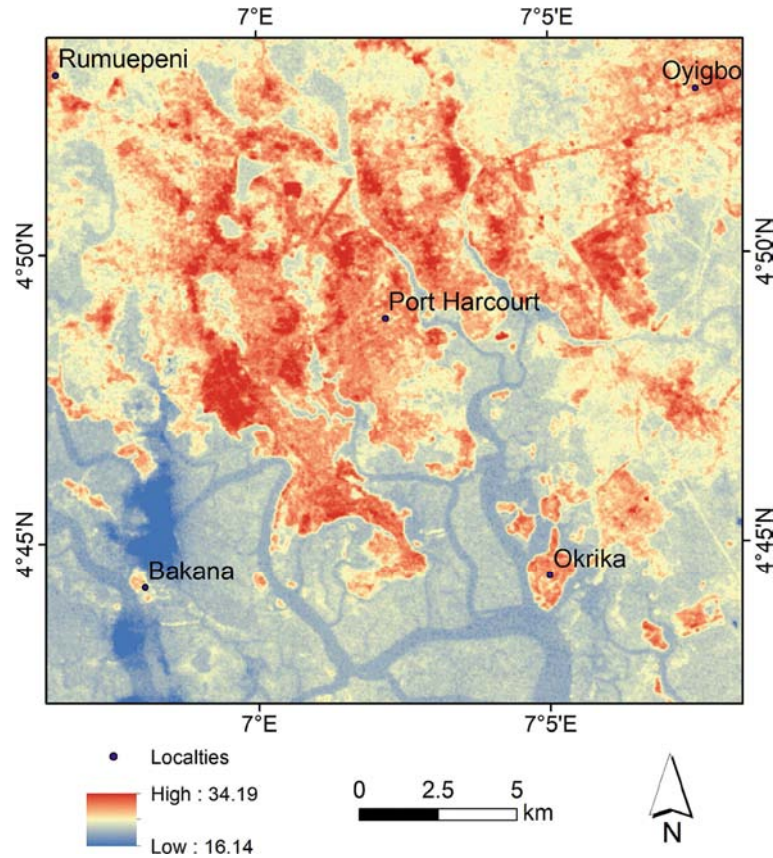


**Figure 5.** Land Surface Temperature of Port Harcourt Metropolis and Environs, 2003.

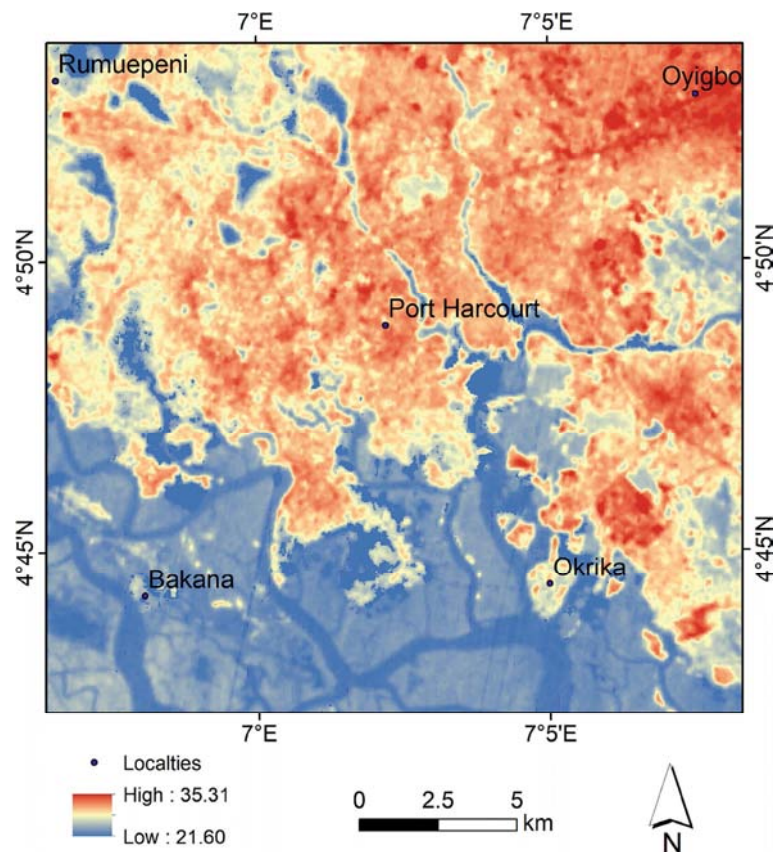


Figure 6. Land Surface Temperature of Port Harcourt Metropolis and Environs, 2018.

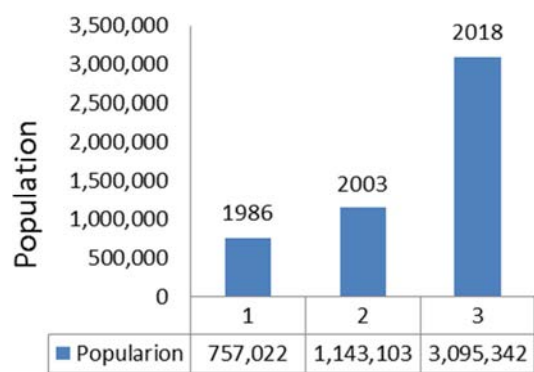


Figure 7. Population of Port Harcourt in 1986, 2003 and 2018.

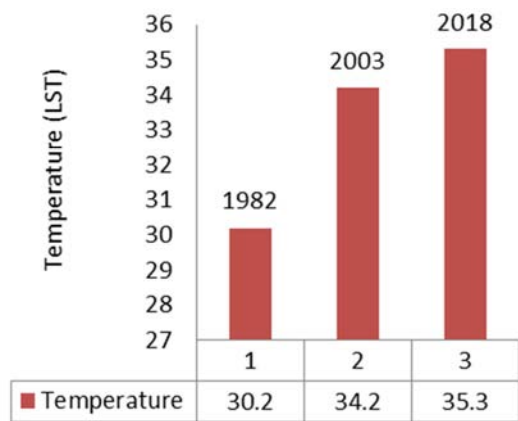


Figure 8. LST of Port Harcourt Metropolis and Environs in 1986, 2003 and 2018.

The trend of population and LST (Figures 7 and 8) were recorded in the city in 1986 with 757,022 persons and temperature of 30.2°C. In 2003 the population was 1,143,109 persons and temperature of 34.2°C; also in 2018 the population rose to 3,095,342 persons with temperature rise of 35.3°C [24]. Notably, high population resulted to accelerated rise in LST due to increased urban pavement materials and human activities. Geo-spatial dynamics of LST in Port Harcourt metropolis and environs since 1986 to 2019 was factored in the performance of population of people modifying the biophysical components of the environment.

4. Conclusion

Population rise has become a major challenge in Port Harcourt City and Environs. In this vein, there is noticeable mass removal of vegetation and other biophysical components of the natural environment that have exposed the land surface of Port Harcourt city and environs. As a result, land surface temperature has increased thereby leading to concentration of urban heat in some segments of the City. Rise in LST will result to heat waves, loss of urban comfort, increased energy consumption, rise in pollution reaction, loss of water quality etc. Therefore, the use of remote sensing of GEE origin has become a vital approach in the study of LST. In the last 33 years, land surface temperature in Port Harcourt metropolis and environs has increased from 30.2°C to 35.3°C with a variation of 5.1°C and current population of 3,095,342 persons. Thus, LST from 1986 to 2018 has remained dynamic

from one section of the city to another characterized by changes in human development activities across the city surfaces. In recent time, north-western (Oyigbo) segment of the city has recorded the highest LST of 35.3°C indicating area with increased concentration of urban fabrics and is susceptible to heat disaster such as heat cramp and stroke. Therefore, development experts should implement tree planting and land management practice that will ameliorate the effect of LST and heat disaster in Port Harcourt metropolis and environs.

## References

- [1] Obinna, V. C., Owei, O. B. and Mark, I. O. (2010) Informal Settlements of Port Harcourt and Potentials for Planned City Expansion. *Environmental Research Journal* Vol. 4. doi: 0.3923/erj.2010.222.228.
- [2] Kerr, Y. H., Lagouarde, J. P., Nerry, F. and Ottele, C. (2000). Land surface temperature retrieval techniques and applications. In D. A. Quattrochi, & J. C. Luvall (Eds.), *Thermal remote sensing in land surface processes* (pp. 33–109). Boca Raton, Fla. CRC Press. Available from: <https://www.crcpress.com>...
- [3] Nwaerema, P. and Nwagbara, M. O. (2018). Urban Warming in Port Harcourt Metropolis and Environs. *Journal of Geography, Environment and Earth Sciences*, 14 (4), 1-19. doi: 10.9734/JGEESI/2018/41123.
- [4] Voogt, J. A. (2002). Urban heat island. In: Munn, T. (Ed.), *Encyclopedia of Global Change*. Wiley, New York. 660-666. Available from: doi.org/10.1016/S0034-4257(03)00079-8.
- [5] Doick, K. J. and Hutchings, T. R. (2013). Air Temperature Regulation by Trees and Wider Green Infrastructure in Urban Areas: The Current State of Knowledge, Research note 12. Forestry Commission, Edinburgh, UK. Available from: [https://www.forestry.gov.uk/pdf/FCRN012.pdf/\\$FILE/FCRN012.pdf](https://www.forestry.gov.uk/pdf/FCRN012.pdf/$FILE/FCRN012.pdf).
- [6] Environmental Protection Agency [EPA] (2008). Report on the Environment. National Center for Environmental Assessment, Washington, DC; EPA/600/R-07/045F. Available from: <http://www.epa.gov/roe>.
- [7] Patki, P. N. and Pratima, R. A. (2007). Study of Influence of Land Cover on Urban Heat Islands in Pune Using Remote Sensing. *Conference on Emerging Trends in Engineering. Journal of Mechanical and Civil Engineering, Second International*, 39, 39-43. Available from: [www.iosrjournals.org](http://www.iosrjournals.org).
- [8] Nwaerema, P and Weli, V. E. (2018). Urban Warming in Port Harcourt Metropolis and Environs. *Journal of Geography, Environment and Earth Sciences*, 14 (4), 1-19. doi: 10.9734/JGEESI/2018/41123.
- [9] Bokaie, M., Zarkesh, M. K., Arasteh, P. D. and Hosseini, A. (2016). Assessment of Urban Heat Island based on the relationship between land surface temperature and land use/land cover in Tehran. *Journal of Sustainable Cities and Society*, 23, 94-104. doi: 10.1016/j.scs.2016.03.009.
- [10] Zhao-Liang, L., Bo-Hui, T., Hua Wu, A., Huazhong R. C., Guangjian, Y. C., Zhengming W. D., Isabel, F., Trigo, E. F. and José, A. S. (2013). Satellite-derived land surface temperature: Current status and perspectives. *Journal of Remote Sensing and Environment*, 131, 14–37. Available from: <http://www.sciencedirect.com/science/article/pii/S0034425712004749>.
- [11] Ramachandra, T. V.1, Bharath, H. A., Durgappa, S. D. (2012). Land Surface Temperature Analysis in an Urbanizing Landscape through Multi Resolution Data. *Journal of Space Science and Technology*. 1 (1), 1-10. Available from: [http://wgbiis.ces.iisc.ernet.in/energy/paper/stmj\\_lsta/land\\_surface\\_temp\\_analysys.pdf](http://wgbiis.ces.iisc.ernet.in/energy/paper/stmj_lsta/land_surface_temp_analysys.pdf).
- [12] Chiadikobi, K. C., Omoboriowo, A. O., Chiaghanam, O. I., Opatola, A. O. and Oyebanji, O. (2011) Flood Risk Assessment of Port Harcourt, Rivers State, Nigeria. *Advances in Applied Science Research*. 2 (6), 287-298. Available from: [www.pelagiaresearchlibrary.com](http://www.pelagiaresearchlibrary.com).
- [13] Fasote, J. (2007). Assessment of land-use and land-cover changes in Port Harcourt and Obio/Akpor local government areas using remote sensing and GIS approach. Available from: [maxwellsci.com/print/rjees/v3-307-313.pdf](http://maxwellsci.com/print/rjees/v3-307-313.pdf).
- [14] Odu, N. N. and Imaku, L. N. (2013). Assessment of the Microbiological Quality of Street-vended Ready-To-Eat Bole (roasted plantain) Fish (*Trachuristrachurus*) in Port Harcourt Metropolis, Nigeria. *Researcher*, 5 (3): 9-18. Available from: <http://www.sciencepub.net/researcher>.
- [15] Edokpa, D. O. and Nwagbara, M. O. (2017). Atmospheric Stability Pattern over Port Harcourt, Nigeria. *Journal of Atmospheric Pollution*, 5 (1), 9-17. Available from: <http://pubs.sciepub.com/jap/5/1/2/>.
- [16] Ede, P. N and Edokpa, D. O. (2015). Regional Air Quality of Nigeria's Niger Delta. *Open Journal of Air Pollution*. 4, 7-15. Available from: doi: 10.4236/ojap.2015.41002.
- [17] Mmom, P. C and Fred-Nwagwu, F. W. (2013). Analysis of Land use and Land Cover Change around the City of Port Harcourt, Nigeria. Available from: <http://garj.org/garjgrp/index.htm>.
- [18] Happiness, E., Ihueze, H. U. and Victor, U. O. (2007). Land-use and land-cover changes in Port Harcourt and Obio/Akpor Local Government Areas of Rivers State - using remote sensing and GIS approach. Available from: <https://uchenwogwugwu.wordpress.com/.../land-use-and-land-cover-changes-in-port>.
- [19] Hart, M. and Sailor, D. (2009). Quantifying the influence of land-use and surface characteristics on spatial variability in the urban heat island. *Theoretical and Applied Climatology* 95, 397-406. Available from: <https://asu.pure.elsevier.com/.../quantifying-the-influence-of-land-use-and-surface-cha>.
- [20] David, P., Zina, M., Nektrarios, C. and Michael, A. (2017). Online Global Land Surface Temperature Estimation from Landsat. *Remote Sens.* 9 (12), 1208. doi.org/10.3390/rs9121208.
- [21] Hulley, G. C. and Hook, S. J. (2011). Generating consistent land surface temperature and emissivity products between ASTER and MODIS data for Earth science research. *Journal of Transactions on Geoscience and Remote Sensing*. 49, 1304-1315. doi: 0196-2892.
- [22] Wan, Z., Li, L. (2008). Radiance-based validation of the V5 MODIS land-surface temperature product. *Int. J. Remote Sens.* 29, 5373-5395. doi.org/10.1080/01431160802036565.



- [23] Li, Z. L., Tang, H., Wu, H., Ren, H., Yan, G. J., Wan, Z., Trigo, I. F., Sobrino, J. (2013). Satellite-derived land surface temperature: Current status and perspectives. *Remote Sens. Environ.* 2013, 131, 14-37. doi: 10.1016/j.rse.2012.12.008.
- [24] National Population Commission [NPC]. (2017). Administrative Division. Nigeria: Author. Available from: <https://www.citypopulation.de/php/nigeria-admin.php?admlid=NGA033>.